EVOLUTION OF THE UNIVERSE

Swati Antala, Salina Bakshi, Jeffrey Barry, Kevin Chen, Benjamin Hsu, Arpan Patel, Payal Patel, Jena Song, Janelle Trinidad, Brian Wexler

Advisor: Dr. Sean P. Hendrick
Assistant: Jackie Haynicz

ABSTRACT

Observations of specific objects and phenomena in space provide basic fundamental information on the evolution of the universe. Some stars, such as the Sun, will evolve into planetary nebulae, while a larger star will explode as a supernova. Examining planetary nebulae will show the final stage in the evolution of Sun-like stars. The Ring Nebula and the Dumbbell Nebula were observed, and composite constructions of each planetary nebula were created after observation with red, green, and blue filters. It was discovered that the nebulae consisted of hydrogen, double ionized oxygen, neon, and helium. Observations of globular clusters show the evolutionary states of many stars at once. M13 and M56 were the two globular clusters observed. Hertzsprung-Russell diagrams were created for each cluster, portraying the relationship between magnitude and temperature of various stars in a cluster. Due to limited resolution, the diagrams do not show conclusive results, but they do indicate the point where stars leave the main hydrogen-burning stage of evolution. The evolution of galaxies can be represented by a Hubble Tuning Fork, displaying elliptical, spiral, and barred spiral galaxies. Several galaxies were observed and the spiral branch of the Hubble Tuning Fork was created. Examples of galactic mergers were also viewed. The study of each of these phenomena will help shape our perception of the evolution of the universe.

INTRODUCTION

Approximately 13.7 billion years ago, the universe is believed to have originated with the Big Bang. The Big Bang released an incredible amount of energy and matter, and the universe began to rapidly expand. Evidence for this expansion can be seen in the microwave background. After the initial explosion, the matter particles released began to cool down and form hydrogen, helium, and trace amounts of lithium, beryllium, and boron. As the universe cooled down, more galaxies, stars, and planets were created [1]. The galaxies, drawn together by gravity, formed galactic clusters, while stars were continuously created within them. With the formation of our Sun, the Earth and other planets were formed, and life was created on our planet from the atoms in the universe. As Carl Sagan said, “We are all made of stardust” [2]. During supernova events, the elements were released, and these elements constitute all life. Just as life evolves on Earth, stars and galaxies evolve in the universe. The physics of the Big Bang is not well understood, but gravity undoubtedly dominates the dynamics of galaxies, stars, and planets today. Mankind has always been curious about the universe, and it is apparent that the implications of universal phenomena do affect human life. It is for this reason that we chose to turn our telescopes to the sky and try to understand how we got here.

Stars are formed from massive clouds of dust and gas, most of which is hydrogen. Due to gravitational forces, gases and dust can come together and get pulled into a rotating central mass. Because of the pressure, the entire region of gas and dust begins to heat up, forming a protostar. If the protostar contains enough mass, the core of the protostar will reach a point where fusion begins. At this point, the protostar becomes a main sequence star. [3] Stars burn hydrogen into helium for the vast majority of their lives. Once a star burns up its hydrogen fuel, it is left with a core of helium surrounded by a layer of hydrogen. The hydrogen ring moves outward and pushes the outer layers outward as well, causing the star to swell into a red giant. Red giants are cooler than their preceding main sequence stars, and are many times larger. Our own Sun, when swelled to its red giant stage, will extend all the way to Earth's orbit. As the layers expand, the helium core ignites to create carbon and oxygen. The helium burning ends, leaving the carbon and oxygen core, which forms a white dwarf star. The outer layers of gas are then shed, forming the planetary nebula.

Planetary nebulae are primarily composed of hydrogen, oxygen, and helium. The various gases that make up the planetary nebulae account for the colors it displays. For example, a nebula emitting red light contains hydrogen, seen in the form of Balmer beta lines, named as such after Johann Jacob Balmer, who studied hydrogen spectral lines. Aside from variances in color, planetary nebulae also vary in shape (elliptical, round, bipolar, quadrupolar, and point-symmetric). Planetary nebulae are important to astronomers for the reason that the Sun will eventually create a planetary nebula as it becomes a white dwarf star. Observing existing planetary nebulae will provide clues as to what lies in the future of the Sun. When viewed, many nebulae appear in vivid and brilliant colors, and are the most intense on the edges due to the fact that we view the nebula more through the gas on the edges of the nebula. The colors most commonly seen from planetary nebulae are green and red. Colors appear due to the presence of various elementary gases in the nebulae that are highly ionized by ultraviolet energy. The color green indicates the presence of double ionized oxygen, and red is produced by hydrogen Balmer beta lines. Hydrogen Balmer beta lines have a wavelength of approximately 4900 Angstroms. [4] Double ionized oxygen has wavelengths of 4959 and 5007 Angstroms.

Other stars many times more massive than the Sun will meet a different destiny. These stars, due to their behemoth sizes, will undergo supernova explosions. A supernova, the death of a star, is the most violent explosion known to man. As a star's fuel is spent, heavier elements are formed through the process of fusion. In this process, hydrogen fuses to form helium, helium fuses to form carbon and oxygen. Oxygen is fused to form silicon, which then fuses to form iron and some nickel. Fusion in the core ceases when iron and nickel are the only elements present. However, the outer layers of the core still host fusion events. Due to the lack of thermal pressure from the lack of fusion in the core, gravitational forces are able to pull in the outer layers, which collapse upon the core. A violent bounce-back occurs and the inner layers bounce and collide with the inwardly falling outer layers, causing the supernova event. Following this explosive event, there can be a neutron star, a black hole, or no remains at all. The ejected gases move farther and farther away from the core, sweeping up interstellar material and forming a supernova remnant. Supernova remnants expand over hundreds of light years and create the rest of the elements in the periodic table. As the remnants cool down, new stars are born from the dust, energy, and new material in the remnant. The death of one star gives rise to the birth of hundreds more [5].

While supernova events are certainly spectacular in nature, our Sun will not explode. Instead, it will form a planetary nebula. We will examine the Dumbbell Nebula (M27) and the Ring Nebula (M57). The Dumbbell Nebula is located in the constellation Vulpecula, about 1,250 light years away from Earth. Charles Messier first discovered the Dumbbell Nebula in 1764, while searching for comets. Any objects that were not comets, including the Dumbbell Nebula, were assigned numbers in Messier's catalogue. The Dumbbell Nebula was the first of the planetary nebula to be discovered. [6] The Ring Nebula, discovered by Antoinne Darquier in 1779, is located in the constellation Lyra about 2,300 light years away from Earth. [7]

Many stars in the Milky Way galaxy exist in large, gravitationally bound groups of stars known as clusters. Clusters are categorized as open or globular. Open clusters contain a few hundred stars and are not held together tightly by gravity. They exist in the plane of the Galaxy. Globular clusters, on the other hand, are found in a halo around the Galaxy's central bulge. They are more tightly bound and contain 10,000 to 1,000,000 stars. They follow highly eccentric orbits up to hundreds of thousands of light years around the Galaxy. There are 150 to 200 globular clusters in our Milky Way galaxy, and approximately 77 of them are found near the galactic center by the constellations of Sagittarius, Scorpio, and Ophiuchus. Globular clusters contain old stars that are classified as Population II stars, which contain less heavy elements than Population I stars such as the Sun, suggesting that the stars are not second or third generation stars born out of supernovae. [8]

Although the stars of a globular cluster are gravitationally bound around the cluster's center, they are subject to disruptions. Some of the stars escape as they are randomly accelerated and as they experience tidal forces from the parent galaxy, while stellar evolutionary effects and loss of gas contribute to the increasing rate of cluster deflation and mass loss. The globular clusters still in existence represent only a small portion of a once larger population; in the next ten billion years, half of the current clusters in the Milky Way are expected to disappear. [8]

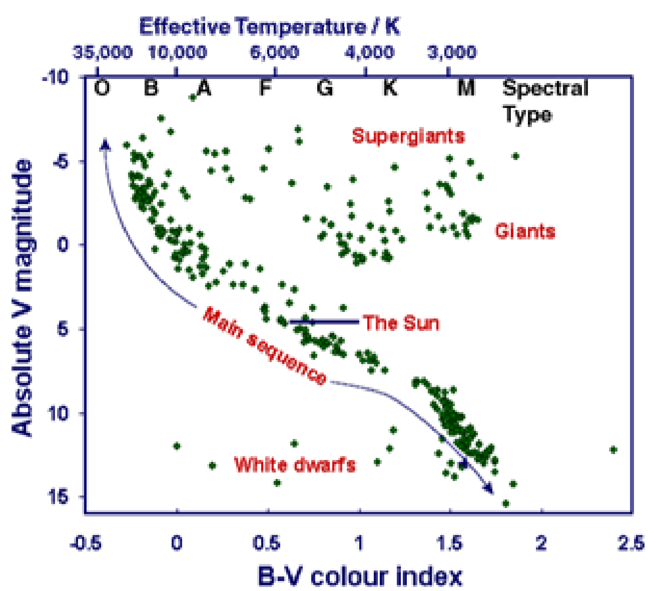

Figure 1: a general H-R diagram

Globular clusters contain some variable stars, which have periodically changing luminosity; they also contain white dwarfs and sometimes even neutron stars. However, the vast majority of globular cluster stars are main sequence stars, stars that fuse hydrogen into helium in the core, and red giants. These stars can be plotted on a Hertzsprung-Russell diagram (Figure 1), a graph plotting the absolute magnitudes of stars versus their temperatures. Lower magnitudes correspond to higher brightness. Vega, in Lyra, for instance, has an apparent magnitude of 0, a full moon has a magnitude of about -10, and the Sun has a magnitude of about -26. Human eyes can see up to a magnitude of 5 or 6, and the Hubble Space Telescope can see up to a magnitude of 30. On the H-R diagram, higher temperatures are plotted towards the left side of the horizontal axis, and lower magnitudes are plotted towards the top of the vertical axis. Temperature can also be expressed by its B-V color index, which is equal to its blue magnitude minus its green magnitude. Since there is a direct correlation between the temperature of a star and its color, the axis portraying temperature on the H-R diagram can be substituted with an axis representing B-V values. Wien's Law describes the correlation between a star's brightest wavelength λ_{peak} in nanometers and its temperature T in Kelvins by the formula

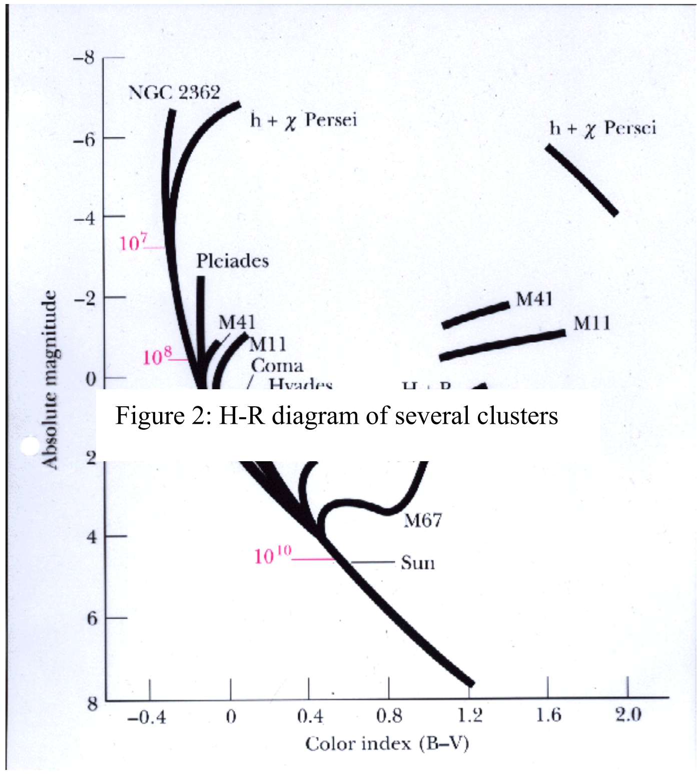

Figure 2: H-R diagram of several clusters

$$(1)\ \lambda_{peak} = \frac{3 \cdot 10^6}{T}$$

This formula shows that stars with high peak wavelengths have low temperatures. Therefore, the horizontal axis not only organizes stars from high to low temperatures; it also organizes stars from blue to red. Main sequence stars appear along a line stretching from the upper left corner to the lower right corner of the H-R diagram. Giants and supergiants are very bright stars and are located towards the top of the diagram. White dwarfs, on the other hand, are dim and are located near the bottom.

The main sequence stars make up the lower right branch of stars on the H-R diagram of a globular cluster (Figure 2), while the red giants appear as the horizontal branch where the main sequence turns to the right. The turnoff point, the point on the diagram where main sequence stars transition into red giants during their evolutionary paths, is an important indication of the age of the cluster. Bluer, more massive stars burn their fuel faster to create greater outward pressure to counter the larger gravitational forces within the star, but stars which consume fuel faster do not live as long. Therefore, redder stars are generally older. The magenta numbers in Figure 2 indicate the relation between turnoff point location and age—older clusters have turnoff points which are lower and farther to the right.

The importance of studying globular clusters can be attributed to their significance in predicting the age of the galaxies they are in. Since a majority of Milky Way globular clusters are believed to have formed early in the history of the Galaxy, determining the ages of globular clusters provides limits on the age of the Galaxy. The age figure is important in understanding the evolution of galaxies, since these clusters are usually as old as the galaxies they are in.

Additionally, determining the distance of the globular clusters can yield various other pieces of information relating to the galaxies in which the globular clusters reside.

The globular clusters M13 and M56 were selected for observation. Because it is one of the brightest and most visually striking clusters in the night sky, M13 is called the "Great Cluster" in Hercules. Compared to M13, M56 is dim and does not have a very concentrated core. We will create H-R diagrams of M13 and M56. The H-R diagrams created will have a vertical axis indicating apparent magnitude in the green wavelength. However, H-R diagrams can also have vertical axes indicating absolute magnitude. By lining up the main sequence from our observations with the main sequence line from an absolute magnitude H-R diagram, we hope to be able to calculate the difference between absolute magnitude, *M*, and apparent magnitude, *m*, so that the distance to the object can be calculated using the distance modulus,

$$(2)\quad m - M = 5\log d - 5$$

The observation and analysis of globular clusters within a galaxy contribute to understanding the evolution of that particular galaxy. It is important to know how galaxies themselves evolve. Our understanding of galaxies can be mostly attributed to the work of Edwin Hubble. While many individuals, such as Charles Messier, Sir William Herschel, Caroline Hershel, and Sir John Herschel observed galaxies, they never understood what these objects truly were. It was only recently that Edwin Hubble realized that they were galaxies. Hubble's pioneering work has also shown that galaxies are found receding away from us, and this laid the foundation of the Big Bang theory. [9] Furthermore, he was essential in contributing to the understanding that cepheid variable stars are used to measure distance because there is a direct correlation between the period of their pulsation and their luminosity. [10] Because of Hubble's work we know that galaxies are massive groups of interstellar matter and stars and usually have masses that are 10^{11} to 10^{13} times that of the Sun. For the most part, they are separated from one another by millions of light years. [11]

Hubble created a Hubble Tuning Fork to classify galaxies and understand galactic evolution to a greater extent. Hubble's Tuning Fork is a way to organize the three major types of galaxies: normal spirals, ellipticals, and barred spirals. Elliptical galaxies branch on the left, followed by normal spiral galaxies, which comprise the top "prong" of the fork; barred spiral galaxies are the bottom "prong" of the fork. From left to right, the elliptical galaxies become flatter, and the normal spiral and barred spiral galaxies become less tightly wound and have smaller cores. Furthermore, in each galaxy, there is more dust and gas as we move from left to right. [12], [13] Hubble thought that galaxies evolved from elliptical shapes to spiral shapes but now it is thought that the opposite is true.

Galaxies fall into four morphological categories: normal spiral galaxies, barred spiral galaxies, elliptical galaxies, and irregular galaxies. Normal spiral galaxies are characterized by a bright, large central bulge composed of interstellar matter and by bright spiral arms where new stars are often formed. Hence, the youngest and brightest stars are in this part of a galaxy. The central bulge contains the oldest stars as well as the gas and dust clouds that were present when the stars were born. Barred spiral galaxies have a bar of stars, instead of a bulge, in the middle and spiral arms which start from each end of the bar. The third type of galaxy, the ellipticals, is either flat or shaped like a ball. Because elliptical galaxies have less dust and gas than spiral galaxies, they usually consist of older stars. The last type of galaxy, the irregular galaxies, can have any shape and is usually classified into Type I irregular and Type II irregular. Type I irregular galaxies, like spiral galaxies, have discs and bulges, but unlike spiral galaxies, they do not have spiral arms. Type II irregular galaxies usually form when two galaxies collide. [11], [12].

Galaxies are drawn together by gravity to form galactic clusters. These consist of hundreds of galaxies, hot gas clouds, and dark matter, an undetectable form of matter on the electromagnetic spectrum. [14] We now know that our Galaxy, the Milky Way, is part of a cluster called the Local Group, which contains at least 30 other galaxies. In this group, the Milky Way and Andromeda Galaxies are the largest. [9] The Local Group is part of the much larger Virgo cluster of galaxies. The Andromeda Galaxy, our closest galactic neighbor and the only galaxy to show blue shift, will merge with the Milky Way Galaxy in about ten billion years.

There are two primary theories explaining galactic evolution. The "Collisional Starburst Scenario" is based on the idea that the universe was built from small structures, such as gas clouds and star clusters, and that these structures continuously merged to form larger and larger galaxies. The second theory, the "Central Quiescent Theory", is based on the idea that gravitational potential wells of dark matter pull in normal matter and through this, galaxies formed to their current size at once. [15].

In the attempt to create a Hubble Tuning Fork and understand the evolution of galaxies, pictures of galaxies were photographed. The spiral galaxies, M101 Pinwheel Galaxy, M51 Whirlpool Galaxy, M81 Galaxy, and M64 were photographed. To represent the elliptical galaxies, M86 was chosen. Furthermore, Stephan's Quintet, also known as NGC 7317, was chosen; this target includes an example of each of the three types of galaxies. The goal of the project is to look at these galaxies and create a tuning fork diagram to hopefully glimpse into the beginnings of our universe.

DATA

Drew University's Richey-Chrétien telescope was used to perform observations; this telescope has a 16" (0.41 m) hyperbolic primary mirror and a focal length of 3.28 m, yielding a focal ratio of $f/8$; the field of view of this instrument is 24' x 24'. A Santa Barbara Instrument Group model ST-1001E charged coupled device (CCD) camera is attached at the end of the telescope to take and record the images using the photoelectric effect. When the CCD is activated, photons from the source in the sky hit a metal plate and push electrons into a well, which are then translated into an image. The CCD uses a Kodak KAF 1001-E CCD chip and takes images with a resolution of 1024 pixels by 1024 pixels (approximately one million pixels overall). The telescope also has several filters that are used to isolate specific colors, since the CCD by itself can only analyze sources in grayscale. The filters used for this project were Bessel Photometric red, green, and blue filters, with peak light intensities around 600 nm, 525 nm, and 425 nm, respectively.

In conjunction with the telescope hardware, several software applications were used. These include *The Sky* v. 5.00.004 [2] and *CCD Soft* v. 5.00.093 [3]. The telescope was linked to *The Sky*, which served as an interface for operating the telescope. By selecting any object displayed in *The Sky* the telescope could automatically slew to that target. CCD images were taken and processed with *CCD Soft*.

Observations**:**

Target Name	**R.A.**	**Dec.**	**Angular Size**	**Filter**	**Distance**
Planetary Nebula					
M27	19h 59m 48.7s	22º 43’ 46’’	4.5’	R,G,B	1.25 kly
M57	18h 53m 47.1s	33º 2’ 25’’	1.6’	R,G,B	2.3 kly
Globular Clusters					
M13	16h 41m 52.3s	36º 27’ 39”	12.5’	B, V	25.1 kly
M56	19h 16m 47.6s	30º 11’ 32”	3.6’	B, V	32.9 kly
Galaxies					
M81	9h 55m 52.7s	69º 2’ 53’’	19.4’	None	12 Mly
M101	14h 3m 22.2s	54º 20’ 1’’	14.4’	None	27 Mly
M64	12h 56m 54.5s	21º 39’ 44’’	7.9’	None	19 Mly
M86	12h 26m 24.5s	12º 55’ 29’’	6.3’	None	60 Mly
M51	13h 30m 4.2s	47º 10’ 40’’	5.0’	None	37 Mly
NGC 7317	22h 36m 7.3s	38º 58’ 22’’	2.3’	None	345 Mly

Data Reduction:

After receiving the data from the CCD camera, *CCD Soft* was used to reduce the data. Lengthy exposures were taken over a period of several weeks. Because of the inability of the telescope to point at its target with 100% precision, *CCD Soft* was used to align the pictures. The data was then combined using the program’s add, average, or median combine capabilities. This step in data reduction takes all of the aligned exposures of a celestial object and combines them into one master picture file. The program was also used to clean the combined pictures and remove the imperfections caused by dust in the telescope. One way these imperfections were removed was by subtracting sky flats, which are blank pictures taken of the uniform sky at twilight. Dark frames, pictures of the inside of the camera, were subtracted using *CCD Soft* to remove false images on the camera itself. The cleaned pictures were then cropped and resized to emphasize the focus on the selected targets.

RESULTS

Planetary Nebula

In 1764, the first planetary nebula, the Dumbbell Nebula (Figure 3), was discovered by Charles Messier. Classified as M27 in the constellation Vulpecula, the Dumbbell Nebula is encircled by a faint halo over 15’ wide, an angle approximately equal to a quarter of the moon’s angular size and has an intrinsic luminosity about one hundred times that of the Sun. The bright portion of the nebula is expanding at a rate of 6.8”/century. The central star, a hot white dwarf,

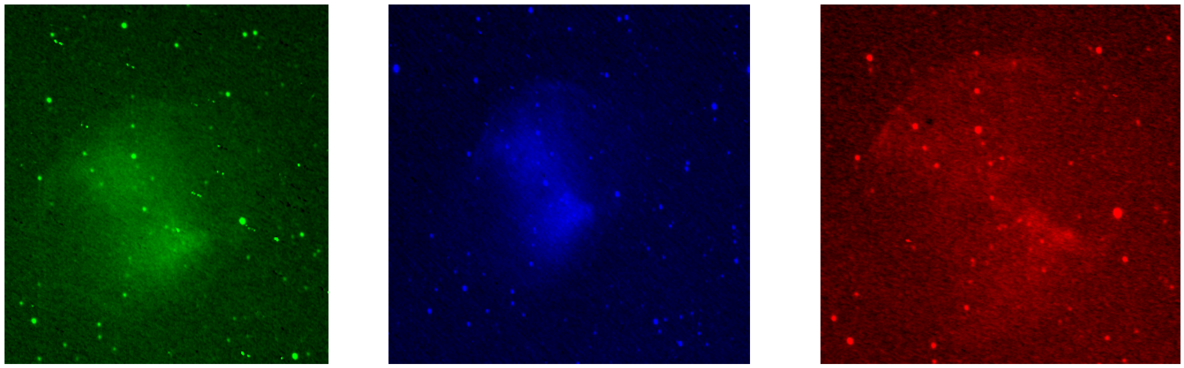

Figure 3: The three pictures above represent green (left), blue (middle), and red (right) images of the Dumbbell Nebula before they were combined to form an image with all three filters.

has a magnitude of 13.5 and is estimated to have a temperature of 85,000 K. Although the age is not definite, the Dumbbell Nebula is estimated to be between 3,000 to 48,000 years old. [4]

Our second target was the Ring Nebula, or M57 (Figure 4), situated in the constellation Lyra and discovered in 1779 by Antoine Darquier de Pellepoix. Pellepoix described the nebula as "a dull nebula, but perfectly outlined; as large as Jupiter and looks like a fading planet." Scientists are unable to come to a general consensus regarding the shape of the Ring Nebula. While some scientists believe that it has a cylindrical shape, others believe that it consists of a ring of material emitting bright light around a central star. The central star is a planet-sized white dwarf that will end its life as a black dwarf, a white dwarf that is no longer active. There is also much ambiguity regarding the distance of the nebula which is estimated to range from 1400 light years to 5000 light years. The mass of nebular matter in the Ring Nebula is 0.2 solar masses and has a density of 10,000 ions per cubic centimeter [4].

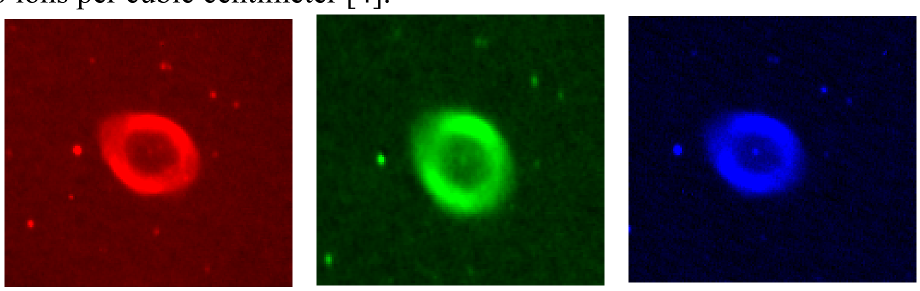

Figure 4: The three pictures above represent red (left), green (middle), and blue (right) images of the Ring Nebula before they were combined to form an image with all three filters.

Both planetary nebulas are elliptical. The chemical composition of the nebulae is determined by analyzing the colors and wavelengths emitted by the nebula. Green signifies the presence of double ionized oxygen, red indicates the presence of hydrogen Balmer beta lines, and blue suggests the presence of helium and neon.

The angular size of the Dumbbell Nebula was found to be 270.12'', and the distance across the nebula was calculated to be 1.25 kilolight years. Using this information and the formula

$$(3)\ s = d \bullet \theta$$

the actual size can be calculated and is found to be 1.637 light years. Similarly, the true size of the Ring Nebula can be calculated. The angular size is 96.88’’and the distance across the nebula was found to be 2.3 kilolight years. Using the same formula mentioned above, the actual size found to be 1.08 light years.

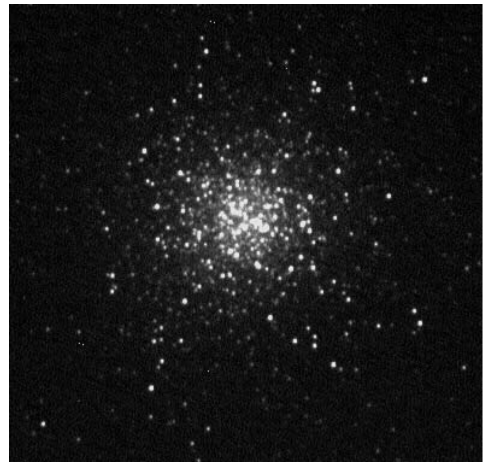

Figure 5: M13, green filtered

Globular Clusters:

The clusters M13 in Hercules and M56 were observed for the analysis of globular clusters. M13, also called NGC 6205, is located in Hercules between the stars η Herculis and ζ Herculis. Astronomers estimated its distance to be roughly 25.1 thousand light years. The entire cluster has an apparent magnitude of 5.8, making it barely visible with the naked eye. Astronomers also estimated that M13 has an apparent diameter of 20.0’, which corresponds to a diameter of 145 light years. The number of stars in the cluster is on the order of hundreds of thousands, and the average concentration of the cluster is about 500 times the star concentration around the Sun. [16]

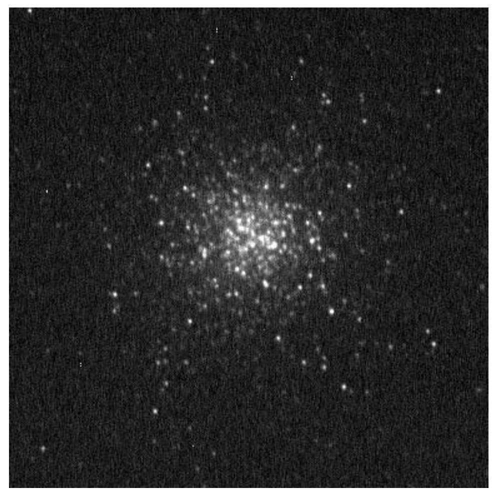

Figure 6: M13, blue filtered

M56, also called NGC 6779, is located in Lyra, between the stars Albireo and Sulafat. Astronomers believe this globular cluster is 32.9 thousand light years away and has an apparent magnitude of 8.3. With an angular size of only 8.8 arc minutes, M56 is more difficult to observe than other clusters such as M13. Its diameter is approximately 85 light years, but only the inner third (3’) is clearly visible. M56 is set apart from other globular clusters because it lacks a bright core. This cluster shows a blue Doppler shift, indicating that it is approaching the Earth. [17]

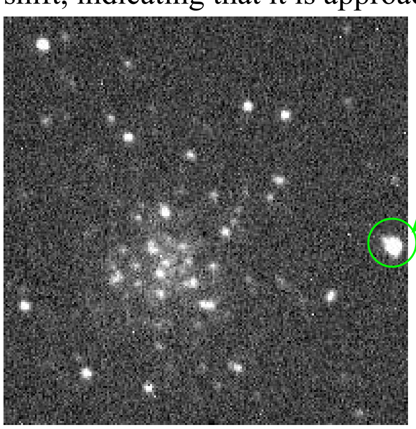

Figure 7: M56, green filtered

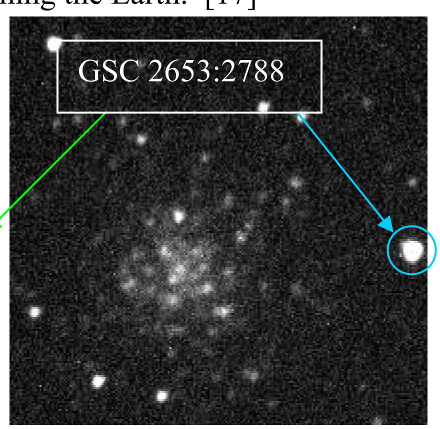

Figure 8: M56, blue filtered

Since the telescope has a viewing angle of 24’ by 24’ and a resolution of 1024 by 1024 pixels, each pixel has an angular size of 1.40625” per pixel. Using this conversion factor, M13’s diameter of 537 pixels was converted to an angular size of $3.66 \cdot 10^{-3}$ radians. The accepted distance to M13 is 25.1 kly, making the cluster's diameter 92 ly. M56's diameter of 155 pixels was converted to an angular size of $1.06 \cdot 10^{-3}$ radians, which at a distance of 32.9 kly is equivalent to a diameter of 35 ly.

This diameter is not necessarily the diameter of the entire cluster; however, it is only equal to the diameter of the observable part of the cluster. Since the telescope used could only see objects up to a magnitude of approximately 20, the outer edges of the cluster may not have been visible in the images taken by the CCD.

After green (Figure 5) and blue (Figure 6) pictures of M13 and green (Figure 7) and blue (Figure 8) pictures of M56 were taken, 25 to 50 stars were picked out of the green and blue images and labeled. For each star, a blue light magnitude B and a green light magnitude V were found using a nearby reference star with B and V values taken from the Tycho Catalogue. M13's reference star was GSC 2588:1662 (not shown in pictures), a star from the Guide Star Catalog, with a blue magnitude of 11.502 and a green magnitude of 11.037; M56's reference star was GSC 2653:2788, with a blue magnitude of 10.403 and a green magnitude of 10.186. Using these values, the blue and green brightness of a star in the cluster could be compared to the reference star's brightness values to find the B and V values of the cluster star. Since green is close to the center of the visible spectrum, the V value was assumed to be equal to the apparent magnitude of each star in the cluster; each star was then plotted in a Hertzsprung-Russell diagram as V versus B – V.

We attempted to locate a turnoff

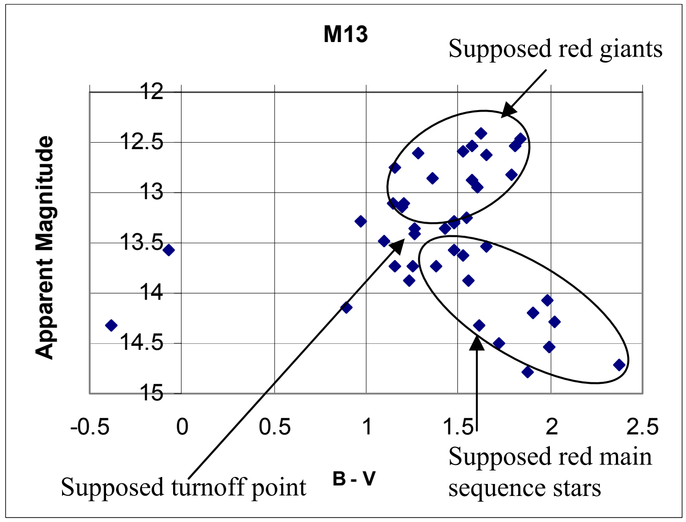

Figure 9: H-R diagram of M13

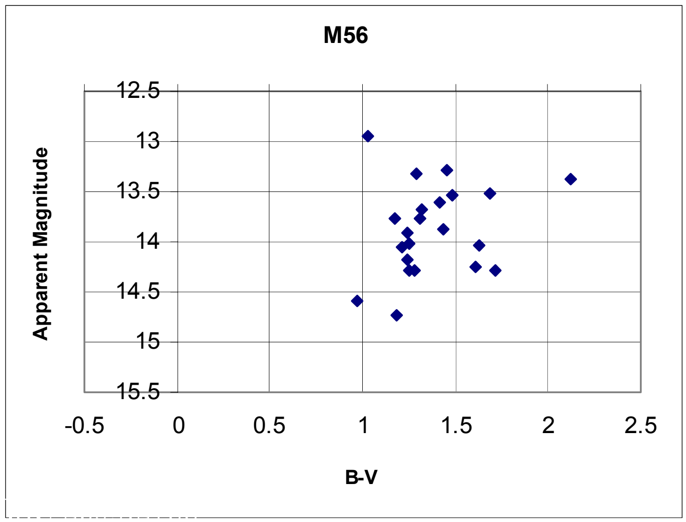

Figure 10: H-R diagram of M56

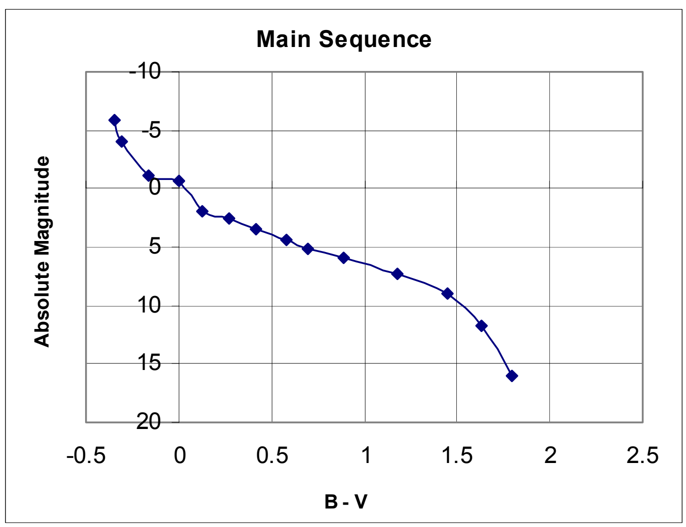

Figure 11: H-R diagram of main sequence

point on the Hertzsprung-Russell diagrams of M13 (Figure 9) and M56 (Figure 10) to estimate the age of the cluster based on the location of the turnoff point on the diagram. Additionally, we tried to line up the main sequence on our own diagram with a main sequence line on a published diagram (Figure 11) in order to find the difference between the apparent magnitude *m* and absolute magnitude *M* of stars in the clusters. This could be used with the equation

$$(2)\ m - M = 5\log d - 5$$

or

$$(4)\ d = 10^{\frac{m-M+5}{5}}$$

to find the distance to the cluster in parsecs. However, no clear turnoff point or main sequence was detected in the Hertzsprung-Russell diagrams.

The fact that the turnoff point in M13 (Figure 9) and M56 (Figure 10) could not be found prevented us from deriving any quantities and making any conclusions about the sources. Initially we believed that M13's turnoff point may be located around a B – V value of 1.3 and an apparent magnitude of 13.3, but this created problems that could not be resolved. If that point had been the turnoff point and all stars to the right and under that point were main sequence stars, the main sequence would not have lined up properly with the actual main sequence. Once the B – V value is greater than 1.5, the slope of the main sequence drops off quickly and becomes a very negative number (Figure 11). The main sequence from B – V = 1.5 to B – V = 2.5 is too steep to line up the M13 diagram with a standard H-R diagram. Consider the two extremes when trying to line up the two diagrams. At the supposed turnoff point of B – V = 1.3, the M13 diagram suggests that *m* = 13.3 and the standard H-R diagram suggests that *M* = 8. Using $m - M = 5\log d - 5$, this yields a distance of 115 parsecs. At the end of the main sequence, where B – V = 1.8, the M13 diagram suggests that *m* = 14.3 and the standard H-R diagram suggests that *M* = 16. This calculation yields a distance of 4.6 parsecs. Both distances are far too small to be realistic, as astronomers believe M13 is 7700 parsecs away. [16]

We developed theories that could explain why our data yielded such erroneous results. The first theory revolved around differences between the filters we used on our telescopes and the filters that were used to find the green and blue magnitudes of reference stars and record them on the Tycho Catalogue. The Tycho Catalogue used a blue and green filter with peak wavelengths (wavelengths of light where white light appears brightest) of 435 and 505 nm [17], respectively. The Bessell photometric filters used on the Drew telescope had a blue and green filter with peak wavelengths of approximately 435 and 525 nm [18], respectively. The difference in green peak wavelength could have caused a noticeable amount of error. Since globular cluster stars are comprised primarily of red (high wavelength) giants and main sequence stars, those stars will appear brighter through a 525 nm filter than through a 505 nm filter. This would make the observed green brightness too high, which in turn would make the green magnitude V too low. Therefore, B – V would be too high.

If this error were corrected and the entire M13 diagram were shifted to the left, it would be easier to line up the M13 main sequence stars with the main sequence line on a standard H-R diagram, since the slope of the main sequence is less negative towards the center of the main sequence. This alone would not solve the problem; however; even if the B – V values were decreased by an entire magnitude, the standard main sequence line would still be too steep and calculated distances would still be too small. For instance, the supposed new turnoff point located at B – V = 0.3 instead of 1.3, which would yield the maximum possible distance based on the data. The M13 diagram suggests that m = 13.3 while the standard H-R diagram suggests that M = 2.8. The equation $m - M = 5\log d - 5$ yields a distance of 1300 parsecs, which, as a maximum distance, is still considerably less than currently accepted values.

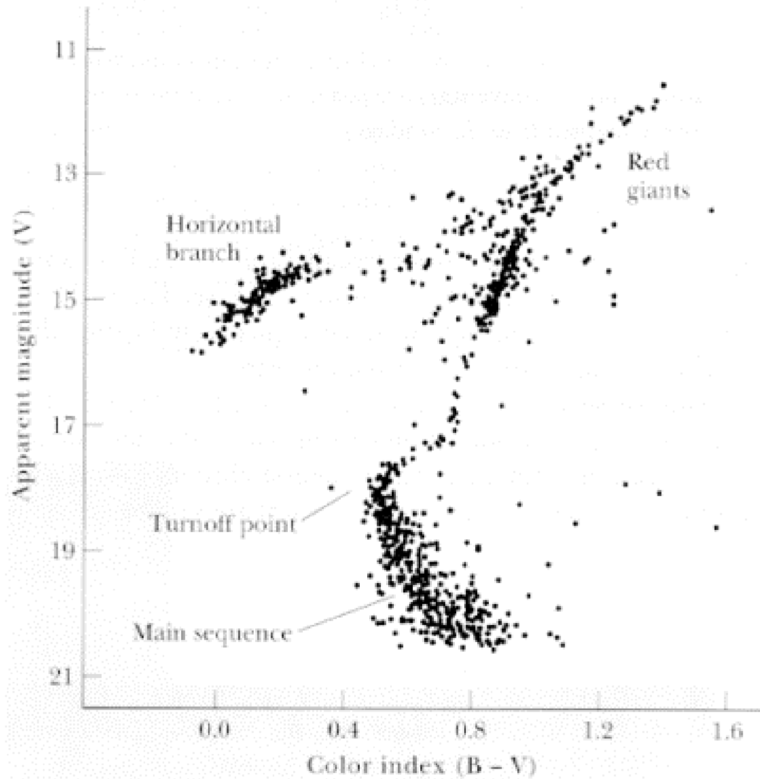

Figure12: H-R diagram of M13 [22]

A second error was also considered. Since the center of M13 is very crowded, only outer stars could be analyzed to extract blue and green magnitudes; it was impossible to pinpoint individual stars near the center. It may be possible that outer stars would be in a different stage of evolution from inner stars, therefore exposing only a section of the globular cluster H-R diagram instead of the entire diagram of red main sequence stars and red giants. This could interfere with the process of lining up M13's main sequence with a standard main sequence.

Ultimately, we discovered that the main source of error is probably the limited power of Drew's telescope. Secondary source research suggests that the main sequence stars in M13 have an apparent magnitude between 18 and 20.5 (Figure 12) [19] Drew's telescope can see objects up to a magnitude 20, but in the presence of giants with magnitudes as low as 11, the giants dominate images and make the faint main sequence stars effectively impossible to see. It turns out, then, that the supposed turnoff point in our M13 diagram (Figure 9) is not a turnoff point at all; every point on the diagram is probably a red giant.

Similarly, the diagram produced from blue and green images of M56 (Figure 10) probably only shows the red giants of the cluster; there is no clear turnoff point in the diagram.

Since M56 is dimmer than M13, it would be even more difficult to observe main sequence stars from the cluster.

In general, the data collected for the globular clusters M13 and M56 yielded inconclusive results. A more powerful telescope with higher resolving power would be required to produce accurate H-R diagrams of the sources.

Galaxies

Our first galactic target, the Pinwheel Galaxy, or M101, dominates its local group. The galaxy has an interesting reaction to the gravity of its neighbors. As seen in Figure 13, the neighboring galaxies' gravitation created M101's characteristic spiral arms and caused the development of bright star forming areas called HII regions throughout its spiral arms. These stars are the second generation of star formation in the galaxy and are essential for prolonging its life. Using distance measurements of 27 million light-years from Cepheid variables and our observations, the diameter of the Pinwheel Galaxy was calculated as 111.4 kly. This is comparable to the Milky Way Galaxy, which has been measured to have a diameter of approximately 100 kly.

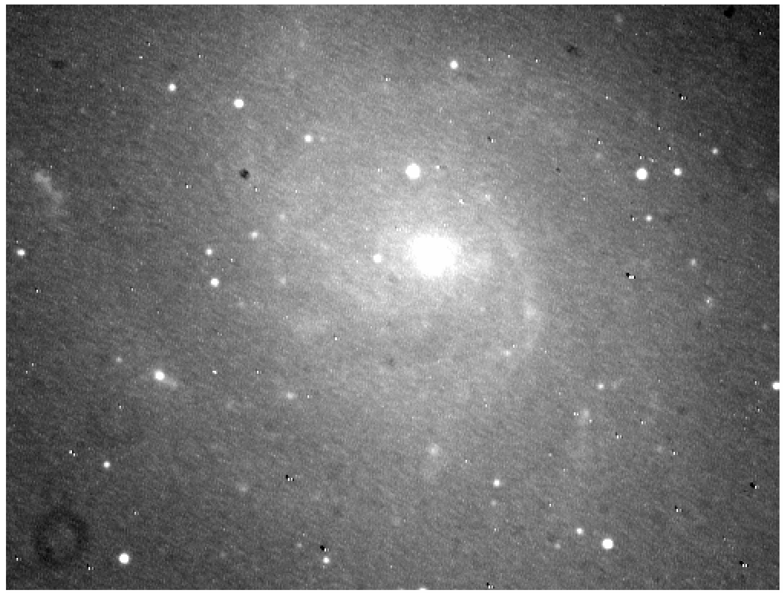

Figure 13: The Pinwheel Galaxy, M101.

Similar to M101, M51 dominates its local group as well. M51, the Whirlpool Galaxy, acts much like a whirlpool on earth does. It is slowly consuming its nearest neighbor, NGC 5195, also called M51B, as seen in Figure 14. As the gases of M51B are pulled into the Whirlpool Galaxy, they become part of the spiral arms of the galaxy. By absorbing its neighbor, the Whirlpool Galaxy is evolving. Recording the evolution of this spiral galaxy can help predict the evolution of our own Milky Way Galaxy, another spiral galaxy. Using a distance measurement of 37 million light-years from SEDS and our observations, the diameter of the Whirlpool Galaxy was measured to be 54.7 kly. NGC 5195 was found to have a

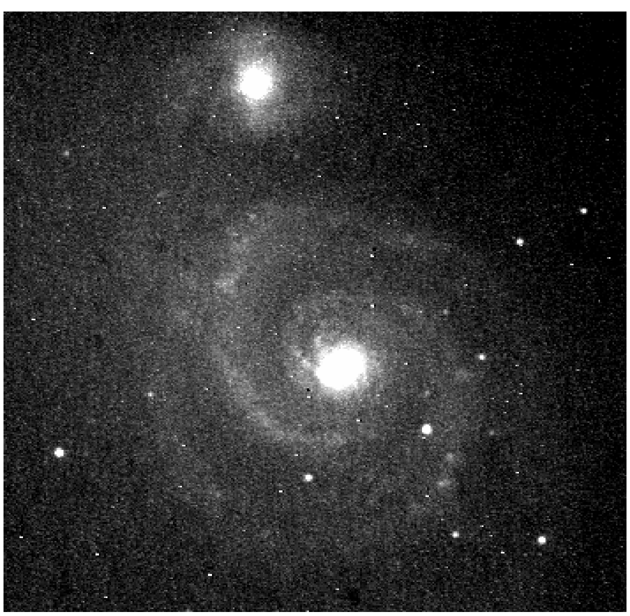

Figure 14: The Whirlpool Galaxy, M51, and its neighbor, NGC 5195 (above).

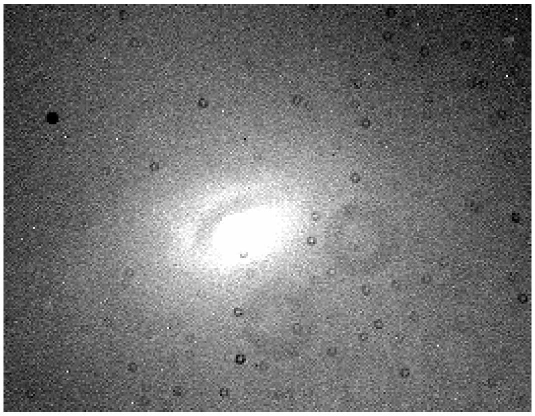

Figure 15: The Black Eye Galaxy, M64

diameter of 9.77 kly.

The Black Eye Galaxy, or M64, is a Hubble type Sb galaxy with a very large dust formation that hides stars behind it. The main spiral pattern in this galaxy is composed of intermediate aged stars. Star formation in the Black Eye Galaxy occurred outside the density gradient and continued while there was enough interstellar matter available. As these stars died out, interstellar matter accumulated from evolved stars, stellar wind, supernovae, and planetary nebula activity. Thus, new stars began to form again. This region appears where the dark dust pattern is located, as seen in Figure 15. It is now believed that this dust lane was caused by the accretion of a former companion, which still has not settled into the main orbital plane of the disk. Using a distance measurement from SEDS of 19 million light-years, the diameter of M64 was found to be 43.8 kly.

Much like M51, our galaxy has combined with others in the past and will do so again in the future; however, it has never combined with any object as massive as our nearest large galactic neighbor, also known as the Andromeda Galaxy, M31. Based on the observations of M31's blueshift, it has been determined that M31 and the Milky Way Galaxy are destined to collide to form an extremely massive galaxy. The shapes of both will change as well. Though the Milky Way and Andromeda Galaxies are currently Hubble types Sbc and Sb respectively, they will form a single elliptical galaxy, and continue moving towards the center of the Virgo Cluster.

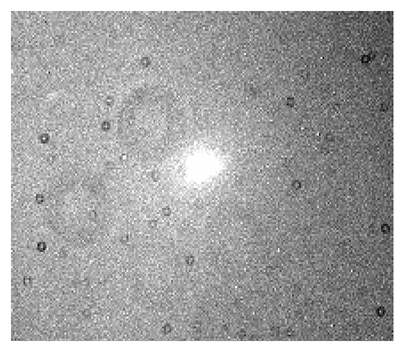

Figure 16: M86

The distances to these and other galaxies made them very difficult to observe. Over distances of millions of light-years, the light emitted from these galaxies was distorted by the earth's atmosphere and interstellar dust. Light pollution from Morristown Airport, New York, Newark further contributed to this distortion. In addition, dirt particles in the telescope itself create imperfections in the image. Normally, sky flats are taken and subtracted from the images to remove these imperfections, but this process did not work effectively for several of the pictures. These obstacles interfered with our capability to create a complete Hubble Tuning Fork and led to the poorer quality in the photographs of M86, Stephan's Quintet, and M81, as seen in Figures 16, 17, and 18.

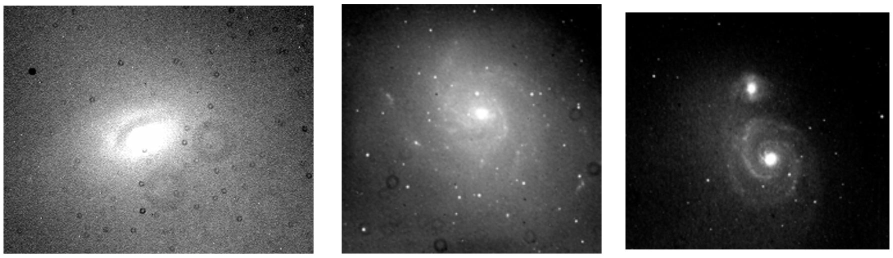

Figure 17: The Evolution of Spiral Galaxies -- M64, Pinwheel, Whirlpool (from left to right)

The evolution of spiral galaxies can be seen through these three pictures. Though the quality of the other three pictures is far from remarkable, they are not altogether useless. They provide examples of the other types of galaxies in the Hubble Tuning Fork. Furthermore, Stephan's Quintet shows the interactions of several galaxies.

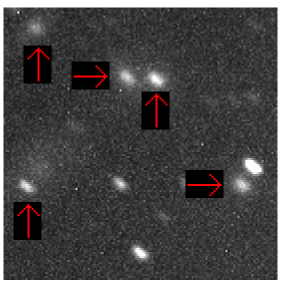

Figure 18: Stephan's Quintet

M86, as seen in Figure 16, is an elliptical galaxy of Hubble type S0 and a member of the Virgo Cluster. Its size was calculated to be 110.3 kly using a distance measurement of 60 million light years from SEDS. Figure 18 depicts Stephan's Quintet, a group of five galaxies. Three of its galaxies are colliding, which creates gravitational distortions in their shapes. The fourth, in the lower right corner of Figure 18, is an elliptical galaxy and gravitationally bound to the group. The fifth is found in the lower left corner, which is not part of the group, but is a much closer object that appears in the foreground of the field. A distance measurement of 280 million light years from SEDS was used to calculate the size of Stephan's Quintet to 179 kly. M81, shown in Figure 19, is a Hubble type Sb spiral galaxy. In the image at right, the spiral is not detectable, but the diameter was still calculable with a distance measurement from SEDS of 12 million light years and found to be 67.9 kly.

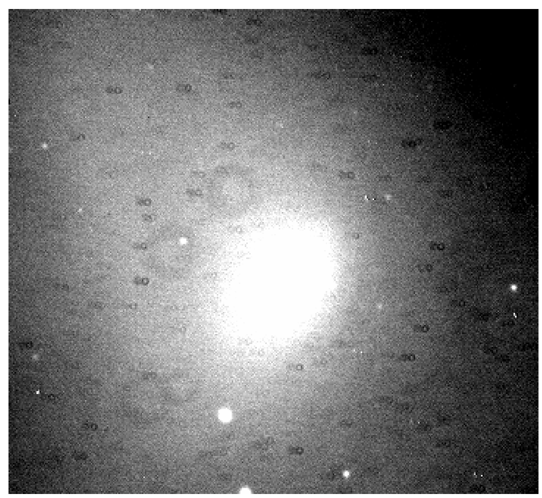

Figure 19: M81

CONCLUSION

Through the observation of such objects in the night sky as planetary nebulae, globular clusters, and galaxies, the evolution of the universe can be further comprehended.

In order to understand the morphology of planetary nebulae, it was necessary to capture various images of these celestial bodies. Using specific color filters, images were successfully created to capture the actual view of nebulae. The color filters chosen for these images were red, green, and blue. The red and green exposures taken produced fair quality images. Though the blue exposures did not produce the same caliber of quality, all the exposures were able to make a satisfactory compilation. These images may be used for further research in observational astronomy; they can give evidence to the spectrum of nebula.

The observations of globular clusters to provide a Hertzsprung-Russell diagram did not meet our expectations. Although we hoped to see a clear main sequence line, a red giant branch, and a turnoff point between the two, the Hertzsprung-Russell diagrams produced from images of M13 and M56 showed only the red giants from each cluster. Because there was no main sequence line in the diagrams to match up with a standard main sequence line, we could not make our own distance calculations; additionally, without a turnoff point on our diagrams, we could not find the age of the clusters. Analysis of M13 and M56 would be possible only with a more powerful telescope that can spot faint main sequence stars, making distance and age calculations possible.

Because galaxies are one of the largest celestial bodies in the universe, studying galactic evolution allows us to begin to understand the evolution of the universe. Although three of our pictures did not provide us with information for the tuning fork, we were able to use the other three in order to understand the evolution of spiral galaxies. Through the M51 Whirlpool Galaxy, the M101 Pinwheel Galaxy, and the M64 Black Eye Galaxy, we were able to follow the progression of spiral galaxies from the Sb stage to the Sc stage; through this we can see that from left to right, they are less tightly wound, have smaller middles, and have more dust and gas.

REFERENCES

[1] "Welcome to the History of the Universe." Penny Press Ltd. 2002. http://www.historyoftheuniverse.com/

[2] Sagan, Carl. "Tribute to Carl Sagan." 5 January 1998. http://www.planetary.org/html/society/tributes/society-sagan-tribute-45.html

[3] "The Life Cycle of Stars." EnchantedLearning.com. 1999. http://www.enchantedlearning.com/subjects/astronomy/stars/lifecycle/

[4] "Atomic Absorption and Emission Spectra." Department of Physics and Astronomy, University of Tennessee. http://csep10.phys.utk.edu/astr162/lect/light/absorption.html

[5] Tyler, Pat. "Supernova." NASA. http://heasarc.gsfc.nasa.gov/docs/snr.html

[6] Frommert, Hartmut and Kronberg, Christine. "M27." SEDS. 9 December 1999. http://www.seds.org/messier/m/m027.html

[7] Frommert, Hartmut and Kronberg, Christine. "M57." SEDS. 15 March 2000. http://www.seds.org/messier/m/m057.html

[8] Frommert, Hartmut and Kronberg, Christine. "Globular Star Clusters." SEDS. 23 November 2003. www.seds.org/messier/glob.html

[9] Guidry, Mike. "Spiral Galaxies." Science and Engineering Research Council. 24 November 1991 http://csep10.phys.utk.edu/guidry/violence/ginfo2.html

[10] Bonnell, Jerry and Nemiroff, Robert. "Astronomy Picture of the Day." 5 August

1997. http://antwrp.gsfc.nasa.gov/apod/ap970805.html
[11] Frommert, Hartmut and Kronberg, Christine. “Galaxies.” SEDS. 25 January 1998. www.seds.org/messier/galaxy.html
[12] Bannister, Nigel. “Hubble Tuning Fork Diagram.” July 2001. http://www.le.ac.uk/physics/faulkes/web/galaxies/o_ga_tuningfork.html
[13] Read, Andy. “Galaxies: Merging Galaxies.” 18 April 2002. http://www.sr.bham.ac.uk/~amr/mergers.html
[14] “Groups and Clusters of Galaxies.” Harvard-Smithsonian Center for Astrophysics. 27 July 2004.
[15] Becker B. Guide to Observing Variable Stars at the Drew University Observatory. May 2003: 1-11.
[16] Frommert, Hartmut and Kronberg, Christine. “M31.” SEDS. 18 September 2003. http://www.seds.org/messier/m/m013.html
[17] Frommert, Hartmut and Kronberg, Christine. “M56.” SEDS. 9 December 1999. http://www.seds.org/messier/m/m056.html
[18] Project Pluto. 2003. http://www.projectpluto.com/gloss/help_4.htm
[19] Javik, Rasmus Flytkjaer; Moeller, Morten and Smedemand, Mikkel. “Globular Cluster M13.” http://www.eso.org/outreach/eduoff/edu-prog/catchastar/CAS2002/cas-projects/denmark_m13_1/image013.gif
[20] “The Properties of Stars.” http://www.jb.man.ac.uk/distance/life/sample/stars/hrdiag.gif
[21] Kauffman: UNIVERSE, Third Edition. W.H. Freeman and Company. 1991. http://aurora.phys.utk.edu/~daunt/diagrams/clusters/Ages.gif http://chandra.harvard.edu/xray_sources/galaxy_clusters.html
[22] Stephens, Tim. “Violent collisions between galaxies fuel star formation, according to new study.” 20 September 1999. http://www.ucsc.edu/currents/99-00/09-20/galaxy.html
[23] The Sky Astronomy Software Manual, Version 5. Software Bisque; 1992-1999.
[24] CCD Soft: CCD Astronomy Software User Guide, Version 5. Santa Barbara Instruments Group and Software Bisque; 2001.
[25] “Astronomy Bessell Photometric Filters.” Glen Spectra. 2003. http://www.glenspectra.co.uk/glen/filters/astronomyfilt.htm
[26] Frommert, Hartmut and Kronberg, Christine. “M27.” 9 December 1999. http:///www.seds.org/messier/m/m027.html
[27] Frommert, Hartmut and Kronberg, Christine. “M51.” 16 January 2000. http://www.seds.org/messier/m/m051.html